DOI: https://doi.org/10.62985/j.huit_ojs.vol26.no2E.401

LOW-COST MONITORING SYSTEM FOR EARLY FAULT DETECTION IN 3S LITHIUM-ION BATTERIES

Chuyen Lam Quang*, Hung Nguyen Huy

Ho Chi Minh City University of Technology and Engineering

*Email: *chuyenlq@hcmute.edu.vn*

Received: 25 April 2026; Revised: 13 May 2026; Accepted: 27 May 2026

ABSTRACT

Lithium-ion batteries are widely used in two-wheel electric vehicles; however, safety risks such as cell imbalance, abnormal current behavior, and localized overheating remain critical concerns during operation. This study experimentally investigates early fault indicators in a 3S lithium-ion battery pack using multi-parameter electrical measurements. Individual cell voltages and pack current were acquired using calibrated instruments under both constant and dynamic load conditions to ensure reliable charging-discharging datasets. The results show that abnormal behaviors, including accelerated voltage drop, cell voltage divergence, and irregular current fluctuations can be detected several seconds before reaching unsafe thresholds. Based on these findings, a low-cost embedded monitoring architecture is proposed for future real-time applications. The system integrates an ESP32 microcontroller, resistor-divider circuits for cell voltage measurement, a bidirectional current sensor, and temperature sensors for continuous monitoring and early fault detection. With its simple design, low cost, and adaptability to both laboratory and practical conditions, the proposed approach offers a promising solution to enhance battery safety in affordable two-wheel electric vehicles.

Keywords: Lithium-ion battery, dynamic discharge load, early fault detection, cell-level monitoring, low-cost battery system.

1. INTRODUCTION

Lithium-ion batteries have become the dominant energy storage solution for two-wheel electric vehicles due to their high energy density, long cycle life, and compact form factor. However, battery-related safety issues remain a major challenge in practical applications, particularly in affordable two-wheel electric vehicles where cost constraints often limit battery management system sophistication. Common failure mechanisms including cell imbalance, abnormal current behavior, and localized thermal rise may develop gradually during operation and escalate into hazardous conditions if not detected early [1]-[3]. In real-world usage, battery packs in two-wheel electric vehicles are subjected to frequent charge–discharge cycling, vibration, and dynamically varying load conditions caused by acceleration, deceleration, and changing road environments. Over time, non-uniform aging among cells leads to divergence in voltage, internal resistance, and thermal characteristics [4], [5]. Conventional low-cost battery protection circuits typically operate at the pack level and react only when predefined voltage or current thresholds are exceeded, offering limited capability for early fault detection.

Recent studies have explored advanced battery monitoring and fault diagnosis techniques, including model-based estimation, machine learning, and distributed battery management architectures [6]-[8]. While these approaches can achieve high diagnostic accuracy, they often require complex models, extensive training data, or high-cost hardware, which restricts their

applicability in low-cost two-wheel electric vehicles. Moreover, many experimental investigations rely on idealized constant-current discharge conditions that do not fully capture fluctuating load behavior encountered in real riding scenarios. To address these limitations, this study focuses on identifying early electrical fault indicators in 3S lithium-ion battery packs under both controlled and realistic operating conditions. Charging and discharging experiments were conducted using calibrated reference measurements to obtain reliable multi-parameter datasets, including individual cell voltages and pack current [9]. In addition, dynamic discharge tests using a practical DC fan load were performed to emulate real-world current fluctuations. Based on experimental observations, a low-cost embedded monitoring architecture is proposed for future real-time implementation, integrating individual cell voltage sensing, current measurement, and cell-level temperature monitoring.

Compared with existing studies that primarily focus on model-based estimation, machine learning algorithms, or complex battery management architectures, this work adopts a measurement-driven experimental approach. The study investigates charging and discharging behavior in 3S lithium-ion battery packs under both constant-current and dynamic load conditions. From the measured voltage and current data, early electrical fault indicators, including cell-voltage divergence and abnormal current variation, are analyzed before unsafe thresholds are reached. Based on these experimental observations, a low-cost, hardware-ready embedded monitoring architecture is proposed for future implementation in affordable two-wheel electric vehicles.

2. EXPERIMENTAL SETUP AND DATA ACQUISITION

2.1. Experimental Battery Model Configuration

The experimental battery pack consists of three commercial 18650 lithium-ion cells connected in series (3S configuration). Each cell has a nominal voltage of 3.7 V and a nominal capacity of 2600 mAh. Prior to testing, the cells were selected and conditioned to ensure similar open-circuit voltages, thereby minimizing inherent imbalance at the beginning of the experiments. Individual cell terminals were made accessible to enable direct measurement of each cell voltage throughout the charging and discharging processes.

2.2. Reference Measurement Instruments

To obtain reliable and high-accuracy experimental data, all voltage and current measurements in this study were acquired using calibrated digital multimeters (VOMs) as reference instruments. The experimental setup is shown in Figure 1, individual cell voltages (V1, V2, and V3) were measured simultaneously using three independent multimeters, while a fourth multimeter was used to measure the pack current during both charging and discharging.

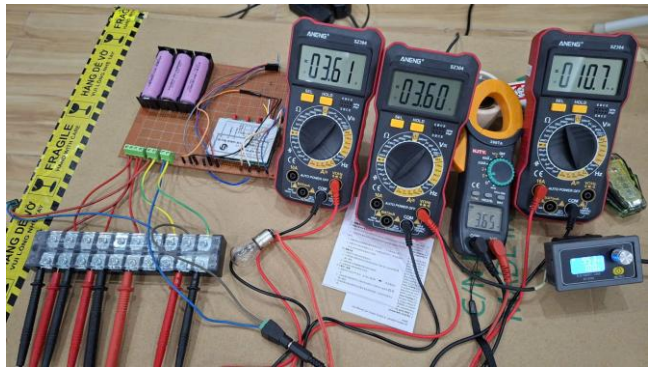

Figure 1. Experimental setup of the battery test system

This reference-based measurement approach was intentionally adopted to eliminate uncertainties related to embedded sensor accuracy, analog-to-digital conversion errors, and firmware-related timing issues. As a result, the collected datasets provide a dependable baseline for analyzing battery behavior and identifying early fault indicators under different operating conditions.

2.3. Charging Setup

Charging experiments were conducted using a standard CC-CV lithium-ion charger with a maximum output voltage of 12.6 V, appropriate for 3S battery packs. During the charging phase, the discharge load was electrically isolated to ensure that the measured current corresponded solely to the charging process.

The battery pack was charged from a partially discharged state to near full capacity. Throughout the charging process, individual cell voltages and pack current were recorded at regular intervals to capture voltage rise characteristics, inter-cell voltage divergence, and current tapering behavior as the battery transitioned from the constant-current (CC) region to the constant-voltage (CV) region.

2.4. Discharging Setup and Load Conditions

Discharging experiments were performed with the charger disconnected. Two types of discharge loads were employed to evaluate battery behavior under both controlled and realistic operating conditions.

2.4.1. Constant-Current Discharge Using Programmable Load

A programmable electronic load was configured to operate in constant-current mode with discharge currents ranging from 0.20 A to 0.23 A. This setup provided stable and repeatable discharge profiles, allowing baseline analysis of voltage decay rate, cell balance behavior, and current stability under laboratory-controlled conditions.

2.4.2. Dynamic Discharge Using Practical Load

A 12 V DC fan was used as a practical dynamic load. Due to mechanical rotation, airflow variation, and load nonlinearity, the fan introduces naturally fluctuating discharge currents, emulating real-world operating conditions.

2.5. Data Acquisition Procedure

During both charging and discharging experiments, individual cell voltages and pack current were recorded simultaneously using the reference multimeters [10]. Measurements were sampled at an effective rate corresponding to the logging interval of the instruments, which was sufficient to capture both gradual trends and short-term variations in electrical behavior.

Each dataset was time-stamped and organized into time-series records for subsequent analysis. Separate datasets were collected for the initial charging stage, near-full charging stage, constant-current discharge, and dynamic-load discharge. This structured data acquisition approach ensured consistent comparison across different operating scenarios.

2.6. Experimental Scope and Limitations

It is important to note that the experimental data presented in this study were obtained using reference measurement instruments rather than an embedded monitoring system. The focus of the experiments was to characterize battery behavior and extract early electrical fault indicators under controlled and realistic load conditions.

Based on the experimental findings, a low-cost embedded monitoring system is proposed for future real-time implementation. The proposed system architecture and

hardware prototype are introduced in a subsequent section, where practical deployment considerations are discussed.

3. RESULTS AND DISCUSSION

3.1. Charging Characteristics and Voltage Evolution

Table 1 illustrates the evolution of individual cell voltages during the charging process of the 3S lithium-ion battery pack. Two distinct charging stages can be clearly identified: the initial charging stage and the near-full charging stage.

Table 1. Initial-stage charging measurements

Index	Data collection				
	Time (s)	V1 (V)	V2 (V)	V3 (V)	Current (A)
1	0	3.10	3.10	3.12	3.25
2	10	3.27	3.30	3.28	3.21
3	20	3.35	3.37	3.35	3.08
4	30	3.39	3.42	3.39	2.92
5	40	3.42	3.45	3.41	2.82
6	50	3.45	3.47	3.44	2.72
7	60	3.47	3.49	3.46	2.65
8	70	3.49	3.51	3.49	2.60

During the initial charging stage, the three cell voltages increase gradually and remain closely aligned, with voltage differences typically below several tens of millivolts. The charging current decreases progressively as the battery transitions from the constant-current region toward the constant-voltage region. This behavior is consistent with the expected CC-CV charging characteristics of lithium-ion batteries and indicates a healthy and balanced charging process.

In the near-full charging stage, the cell voltages approach a plateau, while the charging current decreases slowly to a low level. Although voltage variations among cells become smaller in absolute magnitude, subtle divergence trends can still be observed. These small deviations, while insufficient to trigger conventional protection mechanisms, may serve as early indicators of imbalance development or non-uniform aging when monitored continuously over time.

The charging results demonstrate that cell-level voltage measurements provide valuable insight into battery condition, particularly in the later stages of charging where pack-level monitoring alone may fail to capture early abnormal behavior.

3.2. Discharge Behavior Under Constant-Current Load

Table 2 presents the discharge characteristics of the battery pack under constant-current conditions using the programmable electronic load. In this scenario, the discharge current remains stable, resulting in smooth and repeatable voltage decay profiles across all three cells.

Under the constant-current discharge condition, the measured cell voltages decreased slightly over the 210 s interval. The voltage spread among the three cells was approximately 120 mV at the beginning of the test and approximately 100 mV at 210 s, while the measured current varied from 0.23 A to 0.20 A.

Table 2. Constant-current discharge characteristics using programmable electronic load

Index	Data collection				
	Time (s)	V1 (V)	V2 (V)	V3 (V)	Current (A)
1	0	4.13	4.08	4.20	0.23
2	30	4.07	4.02	4.14	0.22
3	60	4.06	4.01	4.13	0.22
4	90	4.06	4.01	4.13	0.21
5	120	4.05	4.00	4.12	0.21
6	150	4.05	4.00	4.11	0.21
7	180	4.04	4.00	4.11	0.20
8	210	4.04	4.00	4.10	0.20

3.3. Discharge Behavior Under Dynamic Load Conditions

Table 3 illustrates the discharge behavior under dynamic load conditions using a 12 V DC fan. Unlike the case of constant current, the discharge current exhibits natural oscillations due to mechanical rotation, changes in airflow, and the nonlinearity of the load.

Table 3. Dynamic discharge characteristics using DC fan load

Index	Data collection				
	Time (s)	V1 (V)	V2 (V)	V3 (V)	Current (A)
1	0	3.63	3.62	3.67	0.380
2	30	3.66	3.64	3.69	0.380
3	60	3.64	3.63	3.67	0.400
4	90	3.62	3.62	3.66	0.400
5	120	3.62	3.61	3.66	0.400
6	150	3.61	3.61	3.65	0.407
7	180	3.61	3.61	3.64	0.407
8	210	3.61	3.60	3.64	0.407

These current fluctuations result in small voltage oscillations across the cells, closely resembling real-world operating conditions in two-wheel electric vehicles. Despite the non-ideal nature of the load, the overall voltage trends remain consistent with those observed under controlled discharge, and no measurement instability is observed.

Importantly, abnormal voltage-drop behavior remains distinguishable from normal load-induced fluctuations. Cells with increased internal resistance or initial imbalance exhibit amplified voltage excursions and a higher rate of voltage decline compared to the other cells. This demonstrates that early fault indicators can still be reliably extracted under realistic, dynamically varying load conditions.

3.4. Early Fault Indicators and Detection Capability

Across all experimental scenarios, several early fault indicators consistently emerge prior to reaching unsafe operating limits. These include accelerated voltage drop of individual cells, increasing voltage divergence among cells, and irregular current behavior under dynamic loads.

The experimental results show that such indicators appear several seconds before conventional protection thresholds such as undervoltage or overcurrent limits—are reached. This time margin is critical for enabling preventive actions, such as load reduction, system warnings, or controlled shutdown, particularly in low-cost battery systems lacking advanced protection mechanisms.

Although temperature measurements are not the primary focus of the present experimental dataset, the observed electrical behaviors strongly correlate with known degradation mechanisms, including internal resistance increase and imbalance development. These findings motivate the integration of cell-level temperature monitoring in future real-time implementations to further enhance early fault detection capability.

3.5. Discussion

The results demonstrate that meaningful early fault detection can be achieved through simple electrical measurements without reliance on complex models or computationally intensive algorithms. The combination of cell-level voltage monitoring and current observation provides sufficient sensitivity to detect abnormal behavior under both controlled laboratory conditions and realistic dynamic load scenarios.

The inclusion of dynamic load testing represents a key strength of this study. While constant-current discharge provides a clean baseline for analysis, real-world battery operation is inherently dynamic. The ability to identify early fault indicators under fluctuating load conditions enhances the practical relevance of the findings and supports the feasibility of deploying low-cost monitoring systems in two-wheel electric vehicles.

Overall, the experimental results validate the effectiveness of the proposed approach as a foundation for future embedded implementation. By translating the observed fault indicators into lightweight real-time detection logic, low-cost battery monitoring systems can be developed to improve safety and reliability without significant hardware or computational overhead.

4. PROPOSED EMBEDDED MONITORING SYSTEM

4.1. Design Rationale

Based on the experimental results presented in Section 3, early abnormal behaviors in 3S lithium-ion battery packs can be effectively identified through cell-level voltage deviation, abnormal current behavior, and emerging imbalance trends under both controlled and dynamic load conditions. These findings provide a solid foundation for translating the observed fault indicators into a practical, low-cost embedded monitoring solution suitable for real-time deployment in two-wheel electric vehicles.

Rather than relying on complex model-based estimation or data-intensive machine learning techniques, the proposed system focuses on lightweight sensing and rule-based analysis. This design choice prioritizes affordability, implementation simplicity, and robustness, which are critical requirements for battery systems used in low-cost two-wheel electric vehicles.

4.2. System Architecture Overview

Figure 2 illustrates the proposed embedded monitoring architecture for a 3S lithium-ion battery pack with a nominal voltage of 11.1 V and a maximum charging voltage of 12.6 V. The system is centered on an ESP32 microcontroller, which serves as the main processing and communication unit. The architecture integrates three sensing subsystems: three voltage-sensing channels for individual cell-voltage measurement, one INA226 bidirectional current sensor for pack-current measurement, and three DS18B20 digital

temperature sensors for cell-level temperature monitoring. The measured voltage, current, and temperature data are acquired at a sampling rate of 5-10 Hz for synchronized multi-parameter monitoring during charging and discharging operations.

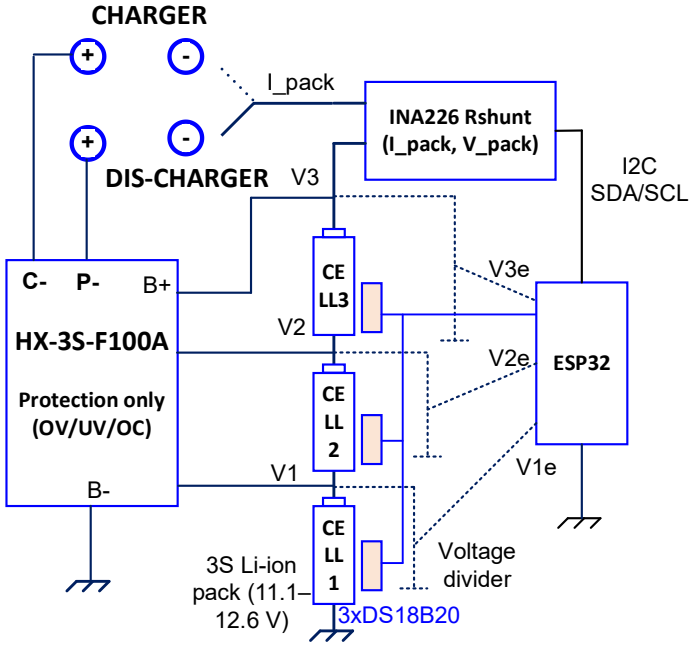

Figure 2. Proposed embedded monitoring system architecture

4.3. Cell Voltage Measurement Module

Individual cell voltages in the 3S battery pack are monitored using high-value resistor-divider circuits. Each divider scales the corresponding cell or stack voltage to a safe input range compatible with the 0-3.3 V analog-to-digital converter (ADC) of the ESP32.

To minimize quiescent current draw and avoid additional loading effects on the battery cells, resistor values in the tens to hundreds of kilo-ohms range are selected. Figure 3 shows the resistor-divider circuit. The output voltage is calculated using Eq. (1). The selected resistor values are summarized in Table 4.

The three divider channels provide scaled voltage signals corresponding to the one-cell, two-cell-stack, and three-cell-stack measurement points.

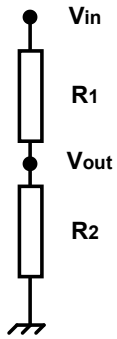

Figure 3. Voltage-divider circuit for cell-voltage measurement

$$V_{out} = V_{ADC} = V_{in} \times \frac{R_2}{R_1 + R_2} \quad (1)$$

where V_{in} is the measured cell or stack voltage, R_1 and R_2 are the divider resistors, and V_{ADC} is the voltage applied to the ADC input of the ESP32.

Table 4. Resistor-divider parameters for cell-voltage measurement

Measurement point	Maximum input voltage (V)	R1 (kΩ)	R2 (kΩ)	ADC input voltage (V)
Pack voltage / 3-cell stack	12.6	300	91	2.93
2-cell stack voltage	8.4	150	75	2.80
1-cell voltage	4.2	39	82	2.85

4.4. Current Measurement Module

Pack current is measured using a digital bidirectional current sensor (INA226) connected in series with the battery pack. The sensor measures the voltage drop across a low-value shunt resistor and provides high-resolution current and bus-voltage data via an I^2C interface.

Digital current measurement avoids many limitations of analog sensing, such as offset drift and noise sensitivity, and allows reliable monitoring of both charging and discharging currents. Abnormal current patterns such as unexpected fluctuations, spikes, or deviations from expected operating profiles can serve as early indicators of load instability or emerging internal faults.

4.5. Temperature Measurement Module

Localized thermal behavior is monitored using DS18B20 digital temperature sensors attached directly to the surface of each battery cell. These sensors provide adequate accuracy to detect gradual temperature rise, inter-cell temperature imbalance, and localized heating effects that often precede hazardous conditions.

Cell-level temperature monitoring complements voltage- and current-based indicators by providing an additional safety dimension. While electrical parameters may reveal early degradation, thermal data offer direct insight into heat generation and dissipation behavior within individual cells.

4.6. Data Acquisition and Processing Strategy

In the proposed implementation, the ESP32 microcontroller acquires voltage, current, and temperature data at a sampling rate of 5-10 Hz. The measured parameters include three cell voltages (V1), (V2), and (V3), pack current, and three cell temperatures (T1), (T2), and (T3). These data are organized as time-series records for synchronized monitoring during charging and discharging operations.

To improve voltage-measurement stability when using high-value resistor-divider circuits, a moving-average filter can be applied to the sampled voltage data. Figure 4 shows the hardware prototype prepared for future real-time implementation, including one ESP32 development board, one INA226 current-sensing module, three voltage-divider input channels, and three DS18B20 temperature sensors for a 3S lithium-ion battery pack with a maximum voltage of 12.6 V.

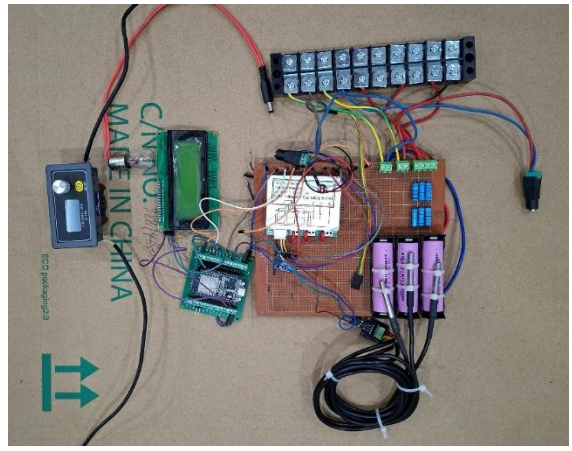

Figure 4. Hardware prototype and future real-time implementation framework

4.7. Proposed Fault Detection Logic

Based on the experimental observations, the proposed fault detection logic evaluates relative deviations instead of relying only on absolute protection thresholds. In this system, lightweight rule-based logic is used to monitor excessive voltage deviation of an individual cell relative to the pack average, accelerated voltage drop rate under load, persistent abnormal current fluctuations, and relative temperature elevation of a single cell compared with the others. When one or more of these indicators exceed predefined deviation or duration limits, the system flags the corresponding operating condition for further warning or protective action.

4.8. Hardware Prototype and Implementation Readiness

A dedicated ESP32-based hardware prototype incorporating voltage divider circuits, an INA226 current sensor, and DS18B20 temperature sensors has been designed and assembled to support future real-time implementation. While the experimental results presented in this study are based on reference measurements, the developed prototype demonstrates the practical feasibility of the proposed architecture.

The prototype serves as a hardware-ready platform for extended validation, long-term cycling tests, and integration with communication interfaces for data logging or warning notification. This staged development approach ensures that experimental insights are translated into a realistic and deployable embedded solution.

5. CONCLUSION AND FUTURE WORK

5.1. Conclusion

This study investigated early fault indicators in 3S lithium-ion battery packs intended for two-wheel electric vehicle applications through experimental charging and discharging tests under both controlled and realistic operating conditions. By employing calibrated reference measurements, reliable multi-parameter datasets were obtained, enabling detailed analysis of individual cell voltage behavior and pack current dynamics.

The experimental results demonstrated that early abnormal behaviors such as accelerated voltage drop, increasing voltage divergence among cells, and irregular current fluctuations can be identified several seconds before reaching unsafe operating thresholds. These findings highlight the limitations of conventional pack-level protection schemes and emphasize the importance of cell-level monitoring for early fault detection.

In addition, the inclusion of dynamic discharge testing using a practical DC fan load enhanced the relevance of the results to real-world operating conditions. The ability to distinguish abnormal electrical behavior from normal load-induced fluctuations confirms that meaningful early fault indicators can be extracted even under non-ideal, field-like conditions.

Overall, the results validate those simple electrical measurements, when properly interpreted, provide sufficient insight for early fault identification without reliance on complex models or computationally intensive techniques. This makes the proposed approach particularly suitable for low-cost battery systems used in affordable two-wheel electric vehicles.

The main contribution of this study lies in bridging experimental fault observation under realistic operating conditions with low-cost, hardware-ready monitoring architecture.

5.2. Future Work

Based on the experimental findings, a low-cost embedded monitoring system has been proposed to enable real-time implementation of the identified fault indicators. Future work will focus on deploying and validating this system using the developed ESP32-based hardware prototype, which integrates individual cell voltage sensing, bidirectional current measurement, and cell-level temperature monitoring.

Further research will include long-term cycling tests to evaluate system performance under extended operating conditions and to investigate the relationship between early fault indicators and battery state-of-health degradation. Additional fault scenarios, such as sustained overload, environmental temperature variation, and mechanical vibration, will also be considered to enhance robustness.

Future developments will also explore on-board protective actions, including automated load disconnection, warning notification, and data logging for predictive maintenance. Extension of the proposed approach to larger battery configurations and integration with existing battery management systems will be pursued to bridge the gap between laboratory experiments and real-world electric vehicle deployment.

REFERENCES

[1] O. Tremblay and L.-A. Dessaint, “Experimental validation of a battery dynamic model for EV applications,” *World Electric Vehicle Journal*, vol. 3, no. 2, pp. 289-298, May 2009, doi: https://doi.org/10.3390/wevj3020289.

[2] T. Zheng, “Fault diagnosis of overcharge and overdischarge of lithium ion batteries,” *Chemical Engineering Transactions*, vol. 71, pp. 1453–1458, 2018, doi: https://doi.org/10.3303/CET1871243.

[3] L. Yang, F. Liu, F. Li, Z. Chen, J. Wang, L. Gao, F. Xiao, J. Sun, and A. Romagnoli, “Thermal runaway prevention and mitigation for lithium-ion battery-powered electric aircraft: Challenges and perspectives,” *Aerospace Traffic and Safety*, vol. 1, pp. 103-118, 2024, doi: https://doi.org/10.1016/j.aets.2024.12.005.

[4] A. Gao, W. Dong, F. Xu, X. Xu, and L. Fan, “Study on thermal runaway behavior of lithium-ion battery under overcharge using numerical detecting method,” *Journal of Physics: Conference Series*, vol. 2195, no. 1, Art. no. 012017, 2022, doi: https://doi.org/10.1088/1742-6596/2195/1/012017.

[5] B. Zou, L. Zhang, X. Xue, R. Tan, P. Jiang, B. Ma, Z. Song, and W. Hua, “A review on the fault and defect diagnosis of lithium-ion battery for Eletric Vehicles,” Energies, vol. 16, Art. no. 5507, 2023, doi: https://doi.org/10.3390/en16145507.

[6] I. Lalinde, A. Berrueta, J. J. Valera, J. Arza, P. Sanchis, and A. Ursúa, "Thermal runaway in lithium-ion batteries," in *Lithium-Ion Batteries – Recent Advanced and Emerging Topics*, IntechOpen, 2022, ch. 1, doi: https://doi.org/10.5772/intechopen.106539.

[7] Z. B. Omariba, L. Zhang, and D. Sun, "Review of battery cell balancing methodologies for optimizing battery pack performance in electric vehicles," *IEEE Access*, vol. 7, pp. 129335–129352, 2019, doi: https://doi.org/10.1109/ACCESS.2019.2940090.

[8] A. Kampker, B. Späth, X. Song, and D. Wang, "Modelling of battery energy storage systems under real-world applications and conditions," *Batteries*, vol. 11, no. 11, Art. no. 392, 2025, doi: https://www.mdpi.com/2313-0105/11/11/392#.

[9] Y.-U. Na and J.-W. Jeon, "A comparative analysis of thermal runaway trigger methods on lithium-ion pouch batteries for fire investigation," *IEEE Access*, vol. 13, pp. 196284 - 196298, 2024, doi: https://doi.org/10.1109/ACCESS.2024.3447873.

[10] I. N. Haq, E. Leksono, M. Iqbal, F. X. N. Soelami, N. Nugraha, D. Kurniadi, and B. Yuliarto, "Development of battery management system for cell monitoring and protection," in *Proc. IEEE Int. Conf. Electrical Engineering and Computer Science (ICEECS)*, Bali, Indonesia, Nov. 2014, pp. 203–208, doi: https://doi.org/10.1109/ICEECS.2014.7045246.